**ZULFAQAR Journal of Defence Science, Engineering & Technology**
e-ISSN: 2773-5281
Vol. 7, Issue 2 (2024)
DOI: https://doi.org/10.58247/jdset-2024-0702-09
Journal homepage: https://zulfaqarjdset.upnm.edu.my

# THE TWO PHASE GENERALIZED MEAN MODEL BASED ON FUZZY LEVEL SET FOR ROBUST IMAGE SEGMENTATION

**Nurul Asyiqin Mohd Fauzi[a], Mazlinda Ibrahim[b*], Hoo Yann Seong[b], Abdul Kadir Jumaat[c,d], Lavdie Rada[d], Haider Ali[e]**

[a] Pusat PERMATA @ Pintar Negara, Universiti Kebangsaan Malaysia, 43600 Bangi, Malaysia
[b] Centre for Defence Foundation Studies, National Defence University of Malaysia, 57000 Kuala Lumpur, Malaysia
[c] School of Mathematical Sciences, College of Computing, Informatics and Media, Universiti Teknologi MARA (UiTM), 40450 Shah Alam, Selangor, Malaysia
[d] Institute for Big Data Analytics and Artificial Intelligence (IBDAAI), Universiti Teknologi MARA (UiTM), 40450 Shah Alam, Selangor, Malaysia
[e] Biomedical Engineering Department, Bahcesehir University, Besiktas, Istanbul, Turkey
[f] Department of Mathematics, University of Peshawar, Peshawar, Pakistan

**ARTICLE INFO**

**ARTICLE HISTORY**
Received: 10-04-2024
Revised: 30-06-2024
Accepted: 31-07-2024
Published: 31-12-2024

**KEYWORDS**
Variational model
Fuzzy level set
Intensity inhomogeneity
Active contour

**ABSTRACT**

Image segmentation is one of the crucial tasks in medical image processing and computer vision. The goal for image segmentation is to separate the pixels in the image into its constituent parts. Variational model in image segmentation involves formulating image segmentation as an optimization problem. The models seeking a partition of the image into meaningful regions by minimizing or maximizing an energy functional. These models often use geometric information to represent object boundaries. The models involve techniques such as active contours and level set methods. In this paper, the generalized mean model for image segmentation is investigated and modified. The model is a 2D region-based model which utilizes the fuzzy level set method. The model is compared with the active contour without edges model also known as the Chan-Vese for three types of images: without noise, with noise and with sinusoidal intensity inhomogeneity. Based on the numerical results, the generalized mean model obtained higher accuracy, Dice similarity measure, Jaccard and Kappa Index, compared to the Chan-Vese model based on the tested images. The model is useful in medical imaging for disease detection, diagnosis, and treatment planning.

## 1.0 INTRODUCTION

Image segmentation aims to partition an image into several regions based on certain characteristics such as colour, texture, and shapes. There exist several approaches for image segmentation, for example, edge detection and active contour models. Active contour models produce sub-regions with continuous boundaries while edge detection methods such as Sobel and Canny often produce sub-regions with discontinuous boundaries. In addition, edge detection methods highly depend on the threshold value. Therefore, active contour models are preferable in the case of medical image segmentation. Active contour models usually used level set methods to obtain the segmented images. Level set methods are a broader class of techniques used for solving partial differential equations (PDEs) involving evolving curves and surfaces. These methods use a higher dimensional function, so-called the level set function to represent the evolving curve implicitly. The curve's position is determined by the zero-level set function. Level set approaches to implement active contour models for image segmentation are preferable due to its flexibility and convenience.

*Corresponding Author | Ibrahim, M. | mazlinda@upnm.edu.my 

The Chan-Vese (CV) model by Chan and Vese [1] is a region-based active contour model that minimizes an energy function by segmenting images into two regions: foreground and background. The two regions are also known as two phase-based models. The CV model can be realized as a specific instance of a level set formulation for image segmentation. The functional consists of two terms: the fitting term and the regularization term. The fitting term in the Chan-Vese model can be interpreted as the image-based forces that influence the evolution of the level set function. The term responsible for attracting the evolving contour towards object boundaries. Meanwhile the regularization term corresponds to curvature or smoothness terms that help maintain a continuous contour. The regularization term is also known as the length term. The convex formulation for the CV model is presented in Brown et al. [2]. The convex formulation in Brown et al. [2] offers more stability and global optimization but the trade-off is the computational efficiency, memory requirements, and boundary sharpness.

The CV model assumes that the image intensities within each segmented region are constant. This assumption might not hold for images with intensity inhomogeneity where the intensity values vary across one object or features in the image. In addition, the model's performance is sensitive to the initial segmentation contour. Thus, incorrect initialization can lead to inaccurate segmentation results and converge to local minima. In addition, the regularization term in the model can lead to over-smoothing of object boundaries, which may cause loss of fine details. The performance of the CV model depends on the proper selection of the parameters, including those related to the data terms. Finding optimal parameters for different types of images can be challenging. Wali et al. [3] improved the distance regularized level set evolution model (DRLSE) via introducing the fast-computing algorithm using the alternating direction method of multipliers (ADMM). However, in the ADMM, there are four additional parameters which related to the four variables in the model. In addition, the model is having similar issues with the CV model in terms of sensitivity to the initial segmentation contour. Poor initialization of the level set might cause the model to converge for a local minimum especially for images with multiple objects or textures.

Ali et al. [4] proposed a generalized mean model where the arithmetic, geometric and harmonic mean are used as the data fitting term by tuning the parameter $p$ in the generalized mean formula. The model in Ali et al. [4] is solved using zero level set function. The model is expanded to accommodate vector-valued images and multi-phase formulations. In Ali et al. [4], the authors evaluated their generalized mean (GM) model using a grayscale image contaminated with salt and pepper noise at a density of 0.01. Additionally, they applied Gaussian filtering to smooth the level set function. Meanwhile, Oh and Kwak [5] mentioned that the generalized mean of positive numbers can be written as a linear combination of the numbers. However, the application for the generalized mean functional in [5] is in face reconstruction, clustering and object categorization. To overcome the problems with the CV and the model in [4], Rahman et al. [6] proposed a power mean model which extends the work in Ali et al. [4] to segment noisy images and images with outliers. The model utilizes the fuzzy level set to evolve the contour. Fuzzy level set combines the principles of fuzzy logic and level set techniques to enhance the robustness and flexibility of the traditional level set. In fuzzy level set, the method allows for handling uncertainties and partial membership. Partial membership is particularly useful in scenarios where strict binary segmentation might not be appropriate. The fuzzy level set method uses fuzzy membership functions to represent the degree of membership of each point to a particular region.

Fuzzy level set methods allow for smoother and more gradual transitions between segmented regions. According to Krinidis and Chatzis [7], fuzzy level set can help avoid sharp, unrealistic boundaries that traditional level set methods might produce. The fuzzy framework is presented in the joint image segmentation and registration of brain MRI with prior information in El-Melegy and Mokhtar [8]. In addition, Mondal [9] and Mondal et al. [10] introduced a resilient active contour method based on fuzzy energy, which incorporates information from both local and global energy components. Leveraging local information, including spatial distance and pixel intensity, helps manage issues arising from high intensity inhomogeneity and image noise. Furthermore, integrating global information is crucial to prevent adverse outcomes stemming from inadequate initialization. In this paper, we reviewed, investigated and modified the model in Rahman et al. [6]. Based on three test images, we observed that the modified GM model works well without the length term in the functional. Thus, reducing the complexity of the model to determine the optimal pairs of the two parameters in the model: $\mu$ and $p$. The parameter $p$ in the model plays an important role in obtaining the correct segmentation of the images. If the images are clean, any values of $p$ work for segmenting the images. However, increasing the values of $p$

*Corresponding Author | Ibrahim, M. | mazlinda@upnm.edu.my

will produce more accurate segmentation results such as improvement of the boundary detection at the corners of the objects.

The length term, also known as the perimeter term, is a component of the energy functional that encourages the contour to have a minimal length or perimeter. The term contributes to the regularization of the contour shape. By minimizing the contour's length, the model encourages smoother, less convoluted contours. This helps prevent overly complex and jagged contour shapes that might lead to overfitting or inaccurate segmentation results. However, according to Zhang et al. [11], one can use a Gaussian filter to regularize the level set. Following this approach, we replaced the length term in Rahman et al. [6] with the 2D Gaussian convolution filter. In addition, Krinidis and Chatzis [7] also highlighted that when no noise is present in the image, we can use $\mu = 0$ where $\mu$ is the regularization paramater. The modified GM model manages to segment images with intensity inhomogeneity and produces global minimum. Compared to the CV model, the initial guess for the level set must vary to produce the optimal results. Wu et al. [12] improved upon the previous study by Krinidis and Chatzis [7] by integrating a kernel metric capable of accurately detecting boundaries, particularly effective in images affected by noise, outliers, and low contrast. Machine learning approaches, particularly deep learning, such as Li et al. [13], Badawy et al. [14], and Thanh et al. [15] have gained prominence in image segmentation due to their ability to learn complex patterns from data. Convolutional Neural Networks (CNNs) are commonly used for semantic and instance segmentation tasks. Machine learning-based image segmentation methods offer significant advantages, but the methods also come with certain disadvantages and challenges.

First, the machine learning methods, especially deep learning, require large amounts of labelled training data. The process of acquiring and annotating such data can be time-consuming and expensive, particularly when the cost is the main issue in specific problem-based applications. Second, deep learning models used for image segmentation can be complex. This complexity can hinder real-time or resource-constrained applications. Third, overfitting occurs when a model learns to memorize the training data instead of capturing meaningful patterns. This can lead to poor generalization of new and unseen data. Fourth, many machine learning algorithms have hyperparameters that need to be tuned to achieve optimal performance. Finding the right combination of hyperparameters can be a time-consuming process. Fifth, models trained on one dataset might not generalize well to other datasets with different characteristics. Domain adaptation or transfer learning might be needed to make models more versatile. The structure of this paper is as follows: In the second section, an overview of the modified GM segmentation model and algorithm are presented. In the third section, the performance comparison for both models are made using four performance metrics on 2D real and synthetic medical images are presented. Conclusions of this paper are described in the last section.

## 2.0 METHODS

The generalized mean, also known as the power mean or Hölder mean, is a mathematical concept used to calculate a single value that represents the "average" or "central tendency" of a set of numbers. It extends the idea of the arithmetic means to incorporate a parameter denoted as $p$, which allows for different weighting of the individual numbers in the set. The formula for the generalized mean for a continuous function $f(x)$ over an interval $[a, b]$ is as follows:

$$M_p = \left(\frac{1}{b-a}\int_a^b f(x)^p dx\right)^{\frac{1}{p}}$$

For a monotonic increasing function $f(x)$, the functional for the generalized mean can be approximated using:

$$M_p = \int (f(\boldsymbol{x})^2)^p d\boldsymbol{x}$$

### 2.1 Two Phase Generalized Mean (GM) Model for Image Segmentation

Defined an image $I$ on $\Omega \subset \Re^2$, and $\Omega_i \subseteq \Omega$ are disjoint connected open subsets with a piecewise smooth boundary $C$ where $I(x) > 0$ is the intensity value at a certain pixel in which $x = (x_1, x_2)$. The minimization functional for GM model in Rahman *et al.* [6] is expressed as

*Corresponding Author | Ibrahim, M. | mazlinda@upnm.edu.my 

$$J(\emptyset(x), c_1, c_2) = \mu \int_{\Omega} |\nabla\emptyset(x)| dx \int_{\Omega} \alpha(x)(I(x) - c_1)^2[\emptyset(x)]^2 dx + \int_{\Omega} \beta(x)(I(x) - c_2)^2[1 - \emptyset(x)]^2 dx \quad (1)$$

where

$$\alpha(\boldsymbol{x}) = ((I(\boldsymbol{x}) - c_1)^2[\emptyset(\boldsymbol{x})]^2)^{p-1}, \ \ \beta(\boldsymbol{x}) = ((I(\boldsymbol{x}) - c_2)^2[1 - \emptyset(\boldsymbol{x})]^2)^{p-1} \quad (2)$$

The first functional in (1) is the length term to regularize the curve $C$. However, when there is noise in the image, we need $\mu \neq 0$ or the Gaussian filter to minimize the length of $C$. The length term is also known as the total variation term. To maximize the detection of objects, regardless of their size, it's preferable to keep the parameter $\mu$ at a small value. Conversely, when the focus is on identifying larger objects or excluding smaller ones, it's advantageous to set $\mu$ to a larger value. Thus, $\mu$ serves as the scaling parameter. When there is no noise in the image, the value of $\mu$ can be set to zero. Lower value of μ caused crookedness and less smoothing of the boundaries between the foreground and the background in the images. The boundaries appeared irregular and jagged. However, the lower value of μ managed to capture finer details in the images. Meanwhile, for the larger value of μ, the model produced smoother boundaries. In addition, with large μ, the fine details in the images will also smooth out. The fuzzy membership function, $\emptyset(x)$ are defined as follow:

$$\begin{aligned} C \quad &= \{(x_1, x_2) \in \Omega : \emptyset(\boldsymbol{x}) = 0.5\} \\ \text{inside } (C) \quad &= \{(x_1, x_2) \in \Omega : \emptyset(\boldsymbol{x}) > 0.5\} \\ \text{outside } (C) &= \{(x_1, x_2) \in \Omega : \emptyset(\boldsymbol{x}) < 0.5\} \end{aligned} \quad (3)$$

and

$$c_1 = \frac{\int_{\Omega} \alpha(x) \mathrm{I}(x)[\emptyset(x)]^2 dx}{\int_{\Omega} \alpha(x)[\emptyset(x)]^2 dx}, \qquad c_2 = \frac{\int_{\Omega} \beta(x)\ \mathrm{I}(x)\ [1 - \emptyset(x)]^p dx}{\int_{\Omega} \beta(x)\ [1 - \emptyset(x)]^p dx} \quad (4)$$

The original function for the generalized mean is given by

$$J(\emptyset(x), c_1, c_2) = \int_{\Omega} [(I(x) - c_1)^2[\emptyset(x)]^2]^p dx + \int_{\Omega} [(I(x) - c_1)^2[1 - \emptyset(x)]^2]^p dx \quad (5)$$

According to Oh and Kwak [5], the generalized mean of a set of positive numbers can be represented as a non-negative linear combination of its elements. Thus, the functional in (5) is reduced to the functional in (1). By keeping $c_1$ and $c_2$ fixed in (4), then minimized $J(\emptyset(x), c_1, c_2)$ with respect to $\emptyset$ and $\mu = 0$, it becomes

$$\emptyset(x) = \frac{1}{1 + \left(\frac{\alpha(x)(I(x) - c_1)^2}{\beta(x)(I(x) - c_2)^2}\right)} \quad (6)$$

Krinidis and Chatzis [7] noted that in two-phase image segmentation, employing the fuzzy energy excluding the length term and utilizing the Jacobi iteration method results in convergence after precisely one sweep, regardless of the initial model condition.

Based on Rahman *et al.* [6], the updated value of $\emptyset(\boldsymbol{x})$ is used in the Euler-Lagrange equation obtained by minimized $J(\emptyset(\boldsymbol{x}), c_1, c_2)$ with respect to $\emptyset$ and $\mu \neq 0$. The Euler-Lagrange equation is solved by introducing $\tau$ as an artificial time and using fully explicit scheme. The GM segmentation model is summarized in Algorithm 1.

Algorithm 1: Modified GM Segmentation Model

BEGIN
Input: Image, $I$
Output: The segmentation of image, $C: Seg(I(x))$

1. Initialization:

   $I, p, \mu, maxit, \emptyset(x)$

2. For $iter = 1, \ldots\ldots, maxit$

*Corresponding Author | Ibrahim, M. | mazlinda@upnm.edu.my

(a) Update $\alpha(x)$ and $\beta(x)$ using (2).
(b) Update the value of $c_1$ and $c_2$ using (4).
(c) Update $\emptyset(x)$ using (6).
(d) Convolve $\emptyset(x)$ using Gaussian Convolution Function.
3. End For.
4. Compute the segmentation of the image using $\emptyset(x)$.
END

## 3.0 RESULTS AND DISCUSSION

In this section, the numerical results for the Algorithm 1 are compared with the CV model using the build in MATLAB function:

```
B = activecontour(I,mask,500,'Chan-Vese','SmoothFactor',mu_cv)
```

where mask is the initial segmentation of the image and mu_cv is the regularization parameters for the length term in the functional. 500 is the maximum number of iterations. To measure the achievement of the models, the accuracy(a), Dice similarity measures (d), Jaccard (j) and Kappa Index (k) are calculated as follows:

$$a = \frac{\mathrm{TP} + \mathrm{TN}}{\mathrm{FN} + \mathrm{FP} + \mathrm{TP} + \mathrm{TN}}, \qquad d = \frac{2\mathrm{TP} + \mathrm{TN}}{2\mathrm{TP} + \mathrm{FP} + \mathrm{FN}}, \qquad j = \frac{d}{2-d},$$

$$pe = \frac{(\mathrm{TP} + \mathrm{FP})(\mathrm{TP} + \mathrm{FN}) + (\mathrm{FN} + \mathrm{TN})(\mathrm{FP} + \mathrm{TN})}{(\mathrm{TP} + \mathrm{TN} + \mathrm{FP} + \mathrm{FN})^2}, \qquad k = \frac{a - pe}{1 - pe}$$

where

• TP : True positive, • FP : False positive, • TN : True negative, • FN : False negative

The values for the performance metrics are $0 \leq a, d, j, k \leq 1$. The smaller values indicate the models are less accurate and has lower similarity with the ground truth. Thus, we aim for the performance metrics close to or equal to 1. We used $\mu$=0 in (1) for all experiments and varies $p$ to obtain the highest values of the performance metrics.

### 3.1 Test 1: Image without Noise

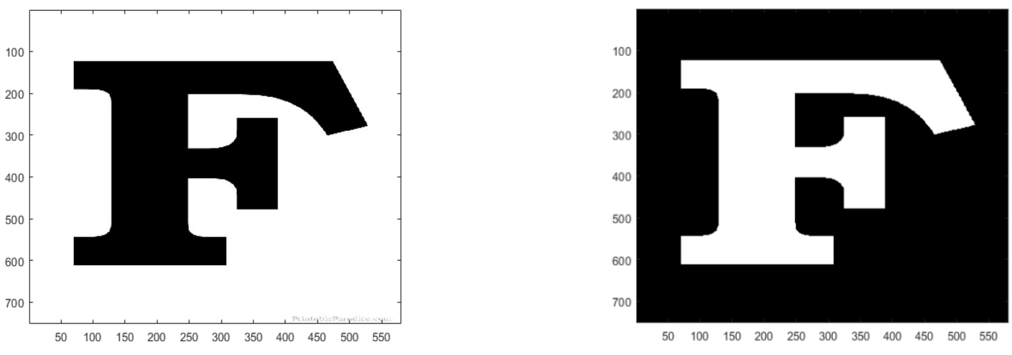

(a) (b)
Figure 1. (a) Test image 1, (b) The ground truth segmentation the image 1

In the first experiment, we tested the models using the letter F as shown in Figure 1 (a). The image has no noise and consists of several sharp corners. The size of the image is 751×580 pixels and 9.6kB. The results for CV models are shown in Figure 2. Different initial mask for the CV model will produce different segmentation results. The optimal initial mask is given in Figure 2 (a) using $\mu\_{cv}$ = 0.1. The difference between the ground segmentation for Test 1 with the CV model is shown in Figure 2(b). The segmentation results clearly struggled with accuracy particularly around the corners of the image.

*Corresponding Author | Ibrahim, M. | mazlinda@upnm.edu.my 

Choosing an appropriate initial contour is crucial to guide the segmentation process. The CV model is non-convex image segmentation model. Thus, segmentation of the image depends on the initialization or the initial state of the active contour. The model used initialization to evolve and segment the image. Thus, we must provide a good initialization which is close to the object boundaries. The CV model has parameters that influence the segmentation result: the weight of the region fitting term and the regularization term $\mu_{CV}$. It's important to note that even though the image in Test 1 is clean and noise-free, the success of the CV model depends on the object's contrast, shape complexity, and the choice of parameters. We had to experiment with different initialization and value of $\mu_{CV}$ to achieve the best segmentation result as shown in Figure 2(b).

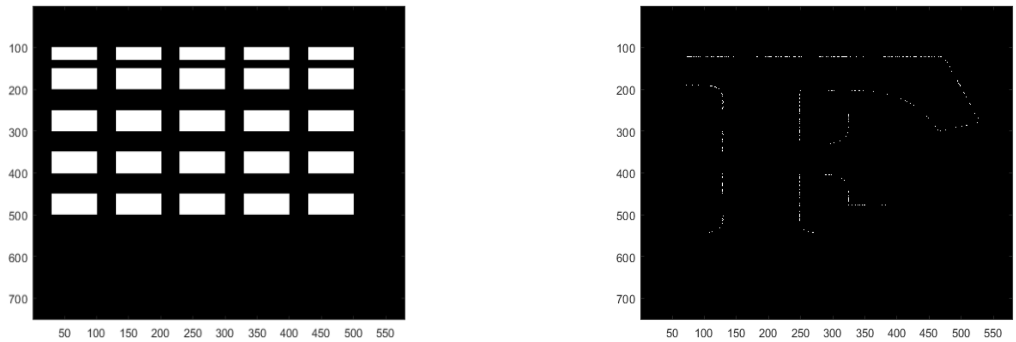


(a) (b)

Figure 2. (a) Initial mask for CV model, (b) The difference between CV model and ground truth segmentation

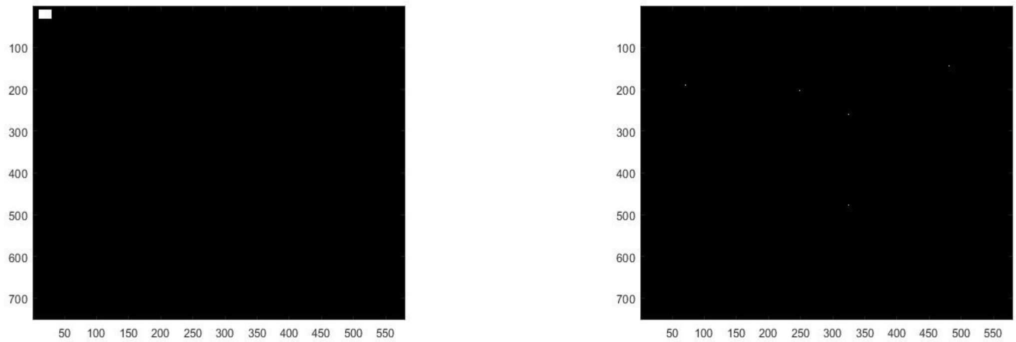


(a) (b)

Figure 3. (a) Initial mask for the GM model, (b) The difference between GM model and ground truth segmentation

Figure 3 shows the results for the GM model. The GM model produce better segmentation results compared to the CV model. The image in Test 1 has well-defined object boundaries and zero intensity variations as shown in Figure 1(a). From Table 1, increasing $\mu_{CV}$ from 0 to 0.1 in the CV model improved the values of the performance metrics. However, the largest values of are given by the GM model using $p$ = 0.5 and 1.0. From this experiment, the GM model outperforms the CV model.

Table 1. Values of the performance metrics for the CV and GM models for Test 1

| Models | $a$ | $d$ | $j$ | $k$ |
|---|---|---|---|---|
| CV model ($\mu_{CV}$=0) | 0.9971 | 0.9947 | 0.9895 | 0.9928 |
| CV model ($\mu_{CV}$=0.1) | 0.9978 | 0.9960 | 0.9919 | 0.9945 |
| GM model ($p$=0.5) | 0.9999 | 0.9999 | 0.9997 | 0.9998 |
| GM model ($p$=1.0) | 1.0000 | 0.9999 | 0.9998 | 0.9999 |

*Corresponding Author | Ibrahim, M. | mazlinda@upnm.edu.my 

### 3.2 Test 2: Image with Low Level of Noise

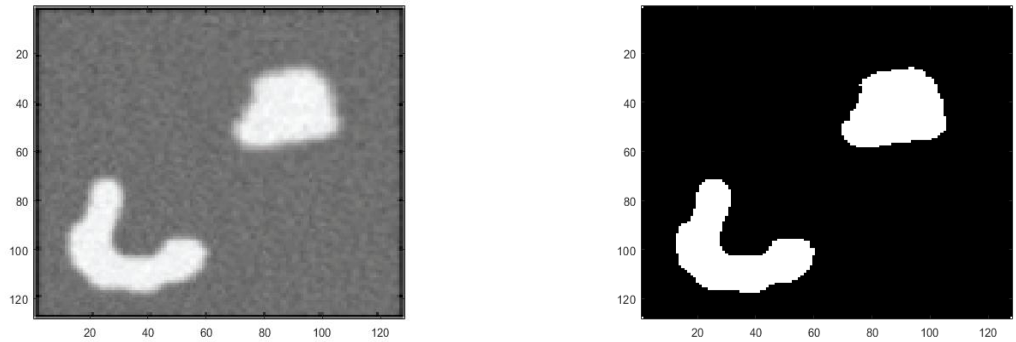

(a) (b)

Figure 4. (a) Test image 2, (b) The ground truth segmentation

In the second experiment, the models are tested for image with noise as shown in Figure 4. The images are from [16] with size 128×128 pixels and 27.4kB. Image segmentation in the presence of noise can be challenging, as noise can introduce errors and affect the accuracy of segmentation algorithms. There exists several image denoising methods such as the Gaussian, median, or bilateral filters which aim to reduce noise while preserving edges in the images. These filters can help create a smoother input image for segmentation. However, in Test 2, we are not using any image denoising methods. The image in Test 2 contains two objects and low level of noise. Similarly, as in Test 1, the initial mask for the CV model must be chosen close to the object boundaries. If the initial mask contains only one square box, then the segmentation results will only produce one object. Thus, we must use two square boxes as the initialization to the CV model.

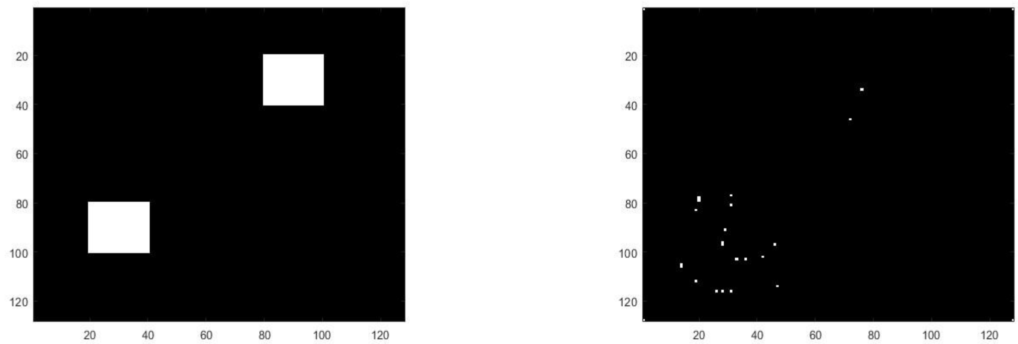

(a) (b)

Figure 5. The results for Test 2 using CV model, (a) Initial mask for the CV model, (b) The difference between CV model and ground truth segmentation

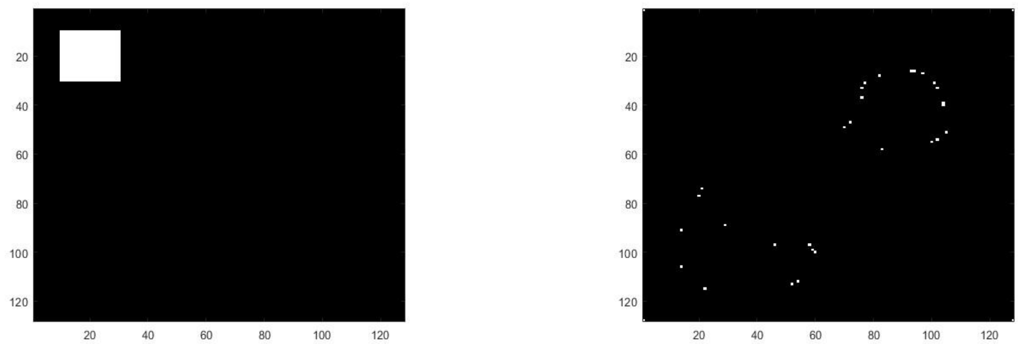

(a) (b)

Figure 6. The results for Test 2 using GM model, (a) Initial mask for the GM model, (b) The difference between GM model and ground truth segmentation

*Corresponding Author | Ibrahim, M. | mazlinda@upnm.edu.my 

The results for the CV and GM models as shown in Figure 5 and 6. The corresponding values of the performance metrics are shown in Table 2. Higher values of a and d are obtained from the GM model using $p = 1$. When $p = 1$, the generalize mean is equivalence to the arithmetic mean. The performance of the CV and GM models are affected when noise is present in the image. Noise introduces variations in pixel intensities, which can lead to challenges in accurately segmenting objects using intensity-based methods like the CV and GM models. The GM model works only for $p \geq 0.6$ with the presence of noise. When $p < 0.6$, the GM model produce inaccurate boundaries of the two objects. Noise led to local intensity fluctuations that do not correspond to actual object boundaries. This causes the GM model to produce inaccurate segmentation of the objects for $p < 0.6$.

Table 2. Values of the performance metrics for the CV and GM models for Test 2

| Models | $a$ | $d$ | $j$ | $k$ |
|---|---|---|---|---|
| CV model ($\mu_{CV}$=0) | 0.9982 | 0.9924 | 0.9850 | 0.9914 |
| CV model ($\mu_{CV}$=0.1) | 0.9985 | 0.9935 | 0.9870 | 0.9926 |
| GM model ($p$=0.9) | 0.9980 | 0.9913 | 0.9828 | 0.9902 |
| GM model ($p$=1.0) | 0.9982 | 0.9921 | 0.9844 | 0.9911 |

### 3.3 Test 3: Image with Sinusoidal Inhomogeneity

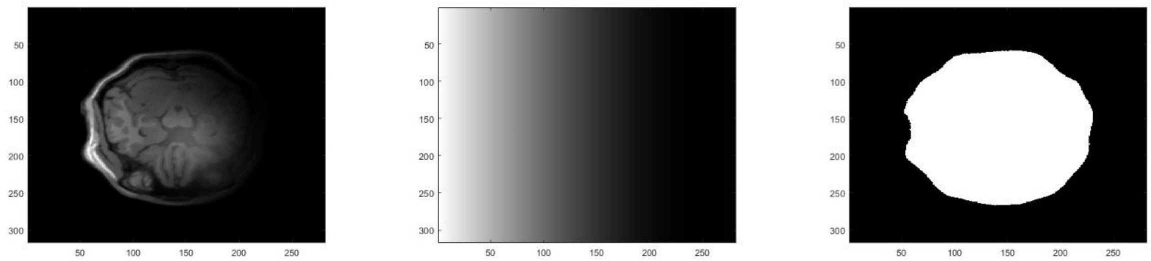

(a) (b) (c)

Figure 7. (a) Images for Test 3, (b)Sinusoidal Intensity Inhomogeneity, (c) Ground Truth Segmentation

We used image from [17] with sizes 317x 281 pixels to test the two models for images with intensity inhomogeneity as shown in Figure 7. Intensity inhomogeneity, also known as intensity bias or shading, refers to variations in image intensities that occur due to uneven illumination, sensor artifacts, or other factors. It can significantly affect image analysis and computer vision tasks, such as segmentation, object detection, and feature extraction. Understanding and correcting intensity inhomogeneity is crucial for obtaining accurate and reliable results in these tasks. The performance of the CV and GM models can be negatively impacted when there is intensity inhomogeneity or uneven illumination present in the image. In Figure 7(b), we add sinusoidal intensity inhomogeneity with amplitude 50 and frequency 0.001 to produce the image in Figure 7(a).

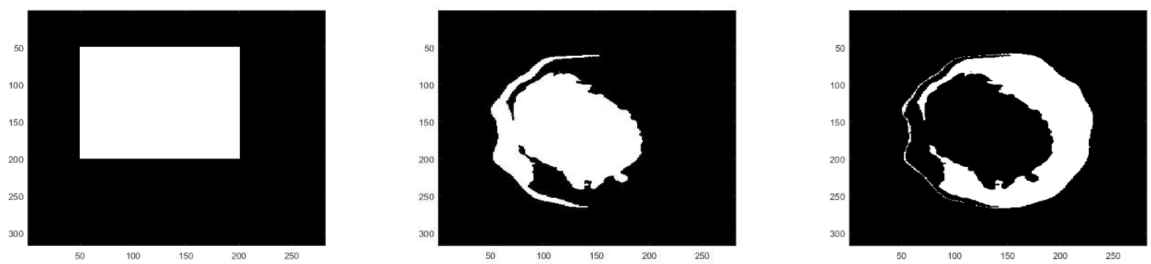

(a) (b) (c)

Figure 8. The results for Test 3 using CV model, a) Initial mask, b) Segmentation result, c) Difference with Ground Truth Segmentation

*Corresponding Author | Ibrahim, M. | mazlinda@upnm.edu.my 

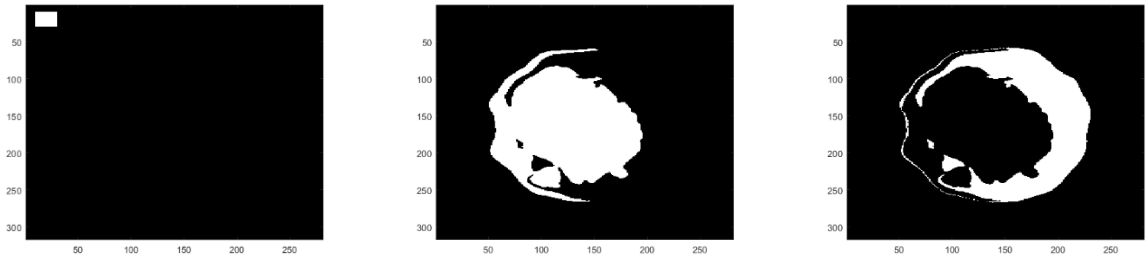


(a) (b) (c)

Figure 9. The results for Test 3 using GM model, a) Initial mask, b) Segmentation result, c) Difference with Ground Truth Segmentation

The results for the CV and GM models are shown in Figure 8 and 9 respectively. Based on the values of the performance metrics in Table 3, we observed that the CV model is at disadvantages when the image contains sinusoidal inhomogeneity as reported in Ali *et al.* [18]. The CV model assumes piecewise constant or smooth intensity values within regions. It struggles to accurately segment images where the intensity varies sinusoidally within a region, as this violates the model's assumptions. However, the GM model incorporates fuzzy logic, which can account for gradual intensity transitions and inhomogeneous intensity distributions within regions. This allows it to handle sinusoidal variations more effectively. In addition, each pixel is assigned a membership value that indicates its degree of belonging to different regions. This adaptive characterization enables the model to better capture complex intensity patterns, like sinusoidal variations, without strict assumptions about homogeneity.

Table 3. Values of the performance metrics for the CV and GM models for Test 3

| Models | $a$ | $d$ | $j$ | $k$ |
|---|---|---|---|---|
| CV model ($\mu_{\_CV}$=0) | 0.8476 | 0.7010 | 0.5397 | 0.6098 |
| CV model ($\mu_{\_CV}$=0.1) | 0.8480 | 0.7021 | 0.5409 | 0.6109 |
| GM model ($p$=0.5) | 0.7515 | 0.4841 | 0.8687 | 0.8968 |
| GM model ($p$=0.7) | 0.8656 | 0.7459 | 0.5948 | 0.6616 |

## 4.0 CONCLUSIONS

In this study, we reviewed, enhanced, and analysed the GM model for image segmentation, demonstrating its capability to function effectively even when μ=0\mu = 0μ=0. We found that the parameter $p$ plays a role like a regularization parameter; however, selecting an optimal $p$ becomes critical in the presence of noise. The GM model was compared to the state-of-the-art CV model using MATLAB's built-in implementation. Through three sets of experiments, we evaluated both models using accuracy, Dice, Jaccard, and Kappa performance metrics. The GM model outperformed the CV model in terms of accuracy and Dice score, particularly for images without noise and for those with intensity in homogeneity. A key advantage of the GM model is its independence from initialization, whereas the CV model's performance is heavily influenced by the initial contour placement. When images exhibit inhomogeneity due to bias fields or acquisition artifacts, the CV model showed significant limitations. Specifically, for objects with varying intensity values, the CV model often segmented either the brighter or darker regions, failing to capture the entire object effectively. Overall, the GM model proved to be more robust, accurate and initialization-independent for segmenting images with intensity in homogeneities, highlighting its advantages over the CV model in such scenarios.

## 5.0 CONFLICT OF INTEREST

The authors declare no conflicts of interest.

## 6.0 AUTHORS CONTRIBUTION

Mohd Fauzi, N. A. (Data curation; Formal analysis; Investigation; Visualisation; Writing - original draft; Writing - review & editing)
Ibrahim, M. (Conceptualisation; Methodology; Validation; Resources; Visualisation; Writing - original draft; Writing - review & editing; Funding acquisition; Project administration; Supervision)

*Corresponding Author | Ibrahim, M. | mazlinda@upnm.edu.my 

Seong, H. Y. (Project administration; Supervision)
Jumaat, A. K. (Project administration; Supervision)
Rada, L. (Conceptualisation; Methodology; Validation)
Ali, H. (Software)

## 7.0 ACKNOWLEDGEMENTS

The research and writing of this work are funded by Ministry of Higher Education of Malaysia and National Defence University of Malaysia under grants RACER/1/2019/ICT01/UPNM/1 and UPNM/2022/GPPP/SG/15.

**List of Reference**

[1] Chan, T., & Vese, L. (1999). An active contour model without edges. In *International conference on scale-space theories in computer vision* (pp. 141-151). Berlin, Heidelberg: Springer Berlin Heidelberg.
[2] Brown, E. S., Chan, T. F., & Bresson, X. (2012). Completely convex formulation of the Chan-Vese image segmentation model. *International journal of computer vision*, *98*, 103-121.
[3] Wali, S., Li, C., Imran, M., Shakoor, A., & Basit, A. (2023). Level-set evolution for medical image segmentation with alternating direction method of multipliers. *Signal Processing*, *211*, 109105.
[4] Ali, H., Shujjahuddin, A., & Rada, L. (2020). A new active contours image segmentation model driven by generalized mean with outlier restoration achievements. *International Journal of Pattern Recognition and Artificial Intelligence*, *34*(11), 2054026.
[5] Oh, J., & Kwak, N. (2016). Generalized mean for robust principal component analysis. *Pattern Recognition*, *54*, 116-127.
[6] Rahman, A., Ali, H., Badshah, N., Zakarya, M., Hussain, H., Rahman, I. U., ... & Haleem, M. (2022). Power mean-based image segmentation in the presence of noise. *Scientific Reports*, *12*(1), 21177.
[7] Krinidis, S., & Chatzis, V. (2009). Fuzzy energy-based active contours. *IEEE Transactions on Image Processing*, *18*(12), 2747-2755.
[8] El-Melegy, M., & Mokhtar, H. (2010, November). Fuzzy framework for joint segmentation and registration of brain MRI with prior information. In *The 2010 International Conference on Computer Engineering & Systems* (pp. 9-14). IEEE.
[9] Mondal, A. (2020). Fuzzy energy based active contour model for multi-region image segmentation. *Multimedia Tools and Applications*, *79*, 1535-1554.
[10] Mondal, A., Murthy, K. R., Ghosh, A., & Ghosh, S. (2016). Robust image segmentation using global and local fuzzy energy based active contour. In *2016 IEEE international conference on fuzzy systems (FUZZ-IEEE)* (pp. 1341-1348). IEEE.
[11] Zhang, K., Song, H., & Zhang, L. (2010). Active contours driven by local image fitting energy. *Pattern recognition*, *43*(4), 1199-1206.
[12] Wu, Y., Ma, W., Gong, M., Li, H., & Jiao, L. (2015). Novel fuzzy active contour model with kernel metric for image segmentation. *Applied Soft Computing*, *34*, 301-311.
[13] Li, Y., Gu, H., Wang, H., Qin, P., & Wang, J. (2022). BUSnet: A deep learning model of breast tumour lesion detection for ultrasound images. *Frontiers in Oncology*, *12*, 848271.
[14] Badawy, S. M., Mohamed, A. E. N. A., Hefnawy, A. A., Zidan, H. E., GadAllah, M. T., & El-Banby, G. M. (2021). Automatic semantic segmentation of breast tumors in ultrasound images based on combining fuzzy logic and deep learning—A feasibility study. *PloS one*, *16*(5), e0251899.
[15] Thanh, D. N., Hai, N. H., Tiwari, P., & Prasath, V. S. (2021). Skin lesion segmentation method for dermoscopic images with convolutional neural networks and semantic segmentation. *Компьютерная оптика*, *45*(1), 122-129.
[16] Ibrahim, M. (2015). *Variational models and numerical algorithms for effective image registration* (Doctoral dissertation, University of Liverpool).
[17] Myronenko, A., & Song, X. (2010). Intensity-based image registration by minimizing residual complexity. *IEEE transactions on medical imaging*, *29*(11), 1882-1891.
[18] Ali, H., Rada, L., & Badshah, N. (2018). Image segmentation for intensity inhomogeneity in presence of high noise. *IEEE Transactions on Image Processing*, *27*(8), 3729-3738.

*Corresponding Author | Ibrahim, M. | mazlinda@upnm.edu.my 